JOURNAL OF BACTERIOLOGY, Jan. 1984, p. 269–276
0021-9193/84/010269-08$02.00/0

Vol. 157, No. 1

# Hairy-Root-Inducing Plasmid: Physical Map and Homology to Tumor-Inducing Plasmids

GARY A. HUFFMAN,[1] FRANK F. WHITE,[1] MILTON P. GORDON,[2] AND EUGENE W. NESTER[1]*

*Department of Microbiology and Immunology[1] and Department of Biochemistry,[2] University of Washington, Seattle, Washington 98195*

Received 18 July 1983/Accepted 10 October 1983

A physical map was constructed for the 250-kilobase plasmid pRiA4b, which confers the virulence properties of a strain of *Agrobacterium rhizogenes* for hairy root disease in plants. The complete *Hin*dIII and *Kpn*I restriction map was determined from a collection of overlapping *Hin*dIII partial digest clones. Homologous regions with two well-characterized plasmids that confer virulence for crown gall disease, plasmids pTiA6 and pTiT37, were mapped on pRiA4b. As much as 160 kilobases of pRiA4b had detectable homology to one or both of these crown-gall-tumor-inducing plasmids. About 33 kilobases of pRiA4b hybridized to the *vir* region of pTiA6, a segment of DNA required for virulence of *Agrobacterium tumefaciens*. Portions of pTiA6 and pTiT37 transferred into plant cells in crown gall disease (T-DNA), shared limited homology with scattered regions of pRiA4b. The tumor morphology loci *tms-1* and *tms-2* from the T-DNA of pTiA6 hybridized to pRiA4b. A T-DNA fragment containing the *tml* and *tmr* tumor morphology loci also hybridized to pRiA4b, but the homology has not been defined to a locus and is probably not specific to *tmr*. A segment of pRiA4b T-DNA which was transferred into plant cells in hairy root disease lacked detectable homology to pTiA6 and had limited homology at one end to the T-DNA of pTiT37.

Hairy root and the related disease, crown gall, occur on susceptible dicotyledonous plants as a growth of callus tissue at a wound infected with *Agrobacterium* spp. (22). Hairy root tumors, unlike crown galls, generally differentiate into roots which proliferate from the callus tissue. Virulence in *Agrobacterium* spp. is conferred by a large bacterial plasmid designated the root inducing (Ri) or tumor inducing (Ti) plasmid (19, 28, 29, 32). Portions of plasmid DNA are transferred into plant cells and integrated into their genome (4, 5, 25, 31, 34). The transferred DNA (T-DNA) encodes genes which control tumor morphology (10, 12, 14, 20). Mutations in these genes result in tumors that form shoots (*tms*), roots (*tmr*), or that grow larger than wild type (*tml*). The T-DNA also encodes genes which direct the synthesis of unique amino acid derivatives called opines, such as octopine (*ocs*), nopaline (*nos*), agropine (*ags*), and agrocinopine (*acs*) (11, 21, 23, 26). Another set of plasmid genes, which is essential for virulence (*vir*), is located outside the T-DNA; i.e., it is not found in the tumor genome.

Ri plasmids and Ti plasmids share homology, which is highly conserved for the *vir* region in the Ti plasmids (33). This finding suggests that the *vir* functions are present in Ri plasmids. Homology between Ri plasmids and the T-DNA of Ti plasmids is limited to the *tms* locus and three other Ti plasmid segments, two of which may encode genes for the synthesis of agropine and agrocinopine (34). The latter three regions of homology are transcribed in hairy root tumor tissue, confirming their presence on the T-DNA of the Ri plasmid and expression in infected plants. Agropine, mannopine, agropinic acid, mannopinic acid, and agrocinopines are present in hairy root tumors (21, 26).

Transposon insertions in the T-DNA of Ri plasmids can eliminate the virulence of *Agrobacterium* spp. on leaves of *Kalanchöe diagremontiana* (30). These insertions fall in a region of the plasmid T-DNA which shares homology with the genome of uninfected *Nicotiana glauca* and which may be the same region having homology to the genome of uninfected *Daucus carota* (25). The cellular homologs of Ri plasmid functions affecting tumorigenicity may or may not be functional in normal plants.

To assist in our understanding of the molecular basis for hairy root induction, we have generated a complete *Hin*dIII and *Kpn*I restriction map of pRiA4b from a *Hin*dIII partial digest clone bank of the plasmid. We also present an analysis of the homology between pRiA4b and two well-characterized Ti plasmids, the octopine-type plasmid pTiA6 and the nopaline-type plasmid pTiT37. Homology to specific Ti plasmid loci was mapped on pRiA4b by DNA hybridization, and the functional relationships between Ri and Ti plasmids implicit in these findings are discussed.

## MATERIALS AND METHODS

**Bacterial strains and plasmids.** Hairy-root-inducing plasmid pRiA4b was obtained from a derivative of the strain A4T (19). Cosmid pHK17 is a wide host range vector constructed from pRK2501 in this laboratory (15). Cosmid pHC79 (13) is a cloning vector derived from pBR322. *Escherichia coli* HB101 (3) was the recipient in all cloning experiments. Plasmids used as probes in hybridization experiments are indicated in the figure legends.

**DNA isolation.** Purified plasmid DNA for cloning and hybridization studies was isolated by the method of Currier and Nester (6). Plasmids were screened by the method of Birnboim and Doly (1).

**Restriction analysis.** Restriction enzymes and reaction conditions were from Bethesda Research Laboratories. Electrophoresis was on 1% agarose in TEA buffer (0.04 M disodium acetate, 0.004 M disodium EDTA, 0.08 M Tris [pH 8.0]) at 1.5 to 2.0 V/cm.

**Cloning methods.** Plasmid pRiA4b was partially digested with *Hin*dIII and ligated at a concentration of at least 100 μg/ml to *Hin*dIII-cleaved pHK17 or pHC79 (T4 ligase;

* Corresponding author.

Bethesda Research Laboratories). Ligated DNA was packaged into phage lambda coats in vitro as described previously (2, 9, 16). Transductants containing pHK17 were selected on L agar (18) containing 10 μg of tetracycline per ml (Pfizer Inc.) and screened for sensitivity to 50 μg of kanamycin per ml (Sigma Chemical Co.), to test for insertional inactivation of the *kan* gene of pHK17. Transductants containing pHC79 were selected on L agar containing 100 μg of ampicillin per ml (Bristol Laboratories) and screened for sensitivity to tetracycline.

**DNA hybridization.** DNA fragments were separated electrophoretically and transferred to nitrocellulose by the method of Southern (24). Radiolabeled probe DNA was prepared either by nick translation of double-stranded DNA (17, 27) with DNase I (Worthington Diagnostics) and DNA polymerase I (New England Nuclear Corp.) from *E. coli* or by fill-in labeling of single-stranded M13 clones (C. Lichtenstein, personal communication) with DNA polymerase I main subunit (Biolabs) and hexadecamer primer for synthesis of hybridization probes (Biolabs). Specific activity of the probes ranged from ca. $5 \times 10^7$ to $2 \times 10^8$ cpm/μg. Hybridization was carried out as described previously (27), except that prehybridization mix containing 6× SSC (1× SSC is 0.15 M NaCl plus 0.015 M sodium citrate), 10× Denhardt solution (7), 20 mM Tris (pH 8), 2 mM EDTA, and 0.1% sodium dodecyl sulfate was left in the hybridization bag, and the boiled probe, adjusted to 6× SSC, was added. High-stringency washes contained 0.3× SSC and 0.1% sodium dodecyl sulfate.

## RESULTS

**Cloning and restriction mapping of pRiA4b.** The Ri plasmid from *Agrobacterium rhizogenes* A4 consists of two dissociable plasmids (32). The component pRiA4a (ca. 170 kilobases [kb]) confers sensitivity to agrocins and the ability to catabolize the opines mannopine, mannopinic acid, and agropinic acid (21). The component pRiA4b (ca. 250 kb) contains all of the functions required for virulence, opine production in tumors, and the ability to catabolize agropine (21, 32). The virulent component has been separated in *Agrobacterium* spp. from the nonvirulent component and composite form for further study. The restriction endonucleases *Hin*dIII and *Kpn*I cleave pRiA4b into 48 and 21 fragments, respectively, with sizes greater than 1.0 kb (Fig. 1).

To map the restriction fragments, we isolated a series of overlapping clones from which the fragment order could be deduced as described by Knauf and Nester (16). The cloned fragments were derived from a *Hin*dIII partial digest of pRiA4b and inserted into one of two vectors. The wide host range cosmid vector pHK17 (12.8 kb) permitted transfer of cloned segments into *Agrobacterium* spp., which would facilitate later experiments such as site-specific mutagenesis of pRiA4b. A smaller cosmid pHC79 (6.43 kb) enabled us to clone larger segments but could not be maintained in *Agrobacterium* spp.

The fidelity of each clone was checked by comparing the restriction fragments of the clone with the restriction fragments of pRiA4b generated by *Kpn*I. *Kpn*I does not cleave either pHK17 or pHC79; therefore for each clone, the *Kpn*I fragment containing the vector is not represented in a *Kpn*I digest of pRiA4b. The band containing the 12.8-kb vector was generally the largest band in each *Kpn*I digest. All other *Kpn*I fragments should match the corresponding pRiA4b fragments, if the cloned segments have no discontinuities. *Kpn*I-digested clones that had more than one electrophoretic band out of alignment with *Kpn*I bands of pRiA4b were discarded. Although it is conceivable that the vector band might comigrate with one of the larger *Kpn*I fragments from the whole plasmid, discontinuous clones of this type would have been detected in most instances because multiple overlapping clones were isolated. In regions in which fewer clones were isolated, the map was confirmed by hybridization as described below. A collection of 47 clones that encompass pRiA4b was assembled in this manner (Table 1).

The *Hin*dIII and *Kpn*I maps of pRiA4b were determined by comparing overlapping clones (Fig. 2). This approach relies on enough clones being isolated to obtain all the overlaps needed to order each fragment. As an example of this analysis, the clones pGH6, pGH19, pGH20, pGH27, pGH38, and pGH42 (Table 1) can be used to define the order of *Hin*dIII fragments 3, 6, 9, 12, 16, and 23 (kilobase coordinates 145 to 185, Fig. 2). The smallest of these clones, pGH20, placed *Hin*dIII fragments 3 and 16 together. Clone pGH27 added *Hin*dIII-12 to one side of fragments 3 and 16. Clone pGH42 placed *Hin*dIII fragments 3, 12, and 6 together; the fragment order was therefore 6-12-3-16. Clone pGH6

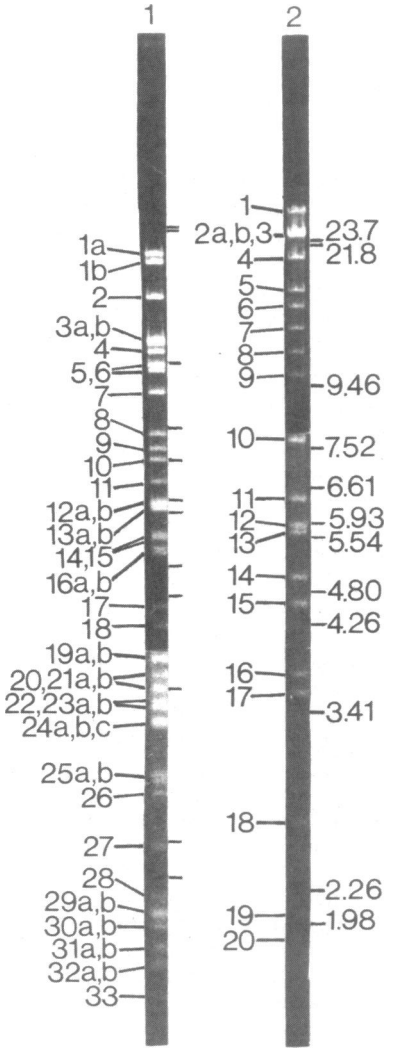


FIG. 1. Electrophoretic patterns of pRiA4b digested with restriction endonucleases *Hin*dIII (lane 1) and *Kpn*I (lane 2). Molecular size standards (kb), marked to the right of each lane, were *Hin*dIII and *Eco*RI fragments of phage lambda DNA.

included all of these fragments plus *Hin*dIII-23, whereas pGH38 contained these fragments plus *Hin*dIII-9 and *Hin*dIII-23. Clone pGH19 contained all of the fragments of pGH38, except for *Hin*dIII-16. This defined fragments 9 and 23 as both being near *Hin*dIII-6 rather than *Hin*dIII-16. The map order was therefore 9-23-6-12-3-16.

An insufficient number of clones were isolated to determine the exact fragment order for the entire plasmid by the method described above. For example, the order of *Hin*dIII fragments 16 and 18 (kilobase coordinate 25) cannot be deduced from the clones listed in Table 1. Insertion of transposons into clones of these regions, which was done for the purpose of mutagenesis and genetic analysis, conveniently resolved most of these ambiguities. Insertions of Tn*3* and Tn*5* were mapped with the restriction enzymes *Eco*RI, *Bam*HI, and *Sal*I in addition to *Hin*dIII and *Kpn*I, providing a more detailed restriction map for much of pRiA4b between kilobase coordinates 210 and 90. The details of the mutational analysis will appear elsewhere. Three pairs of *Hin*dIII fragments were not ordered: 33 and 34 (kilobase coordinate 67), 31 and 21 (coordinate 125), and 27 and 28 (coordinate 190). *Kpn*I fragments 18 and 19 (coordinate 225) also were not ordered.

TABLE 1. *Hin*dIII partial digest clone bank of pRiAb

| Clone | *Hin*dIII fragments of pRiAb | Vector |
|---|---|---|
| pFW | | |
| 3 | 11, 13(doublet), 14, 21, 25, 26, 30, 31, X | pHK17 |
| 6 | 7, 16, 17, 18, 21, 24, 30, 32, X | |
| 22 | 11, 13(doublet), 14, 25, 26, 30, 31, 32, X | |
| 32 | 8, 10, 13, 14, 19, 25, 26, 31, 32 | |
| 41 | 3, 7, 15, 22, 24 | |
| 55 | 4, 5, 20, 24, 29, 33, 34 | |
| 67 | 8, 10, 13, 25, 26, 31, 32 | |
| 72 | 11, 13, 17, 21, 30(doublet), X | |
| 94 | 11, 16, 17, 18, 21, 24, 30(doublet), 32, X | |
| 104 | 7, 15, 16, 17, 18, 22, 24, 32 | |
| pGH | | |
| 6 | 3, 6, 12, 16, 23 | pHK17 |
| 7 | 10, 12, 19, 23 | |
| 8 | 8, 13, 26, 32 | |
| 9 | 1a, 6, 9, 23 | |
| 11 | 1b, 4, 19, 25 | |
| 12 | 1a | |
| 14 | 1a, 2, 21, 31 | |
| 17 | 1b | |
| 18 | 8, 10, 19, 32 | |
| 19 | 3, 6, 9, 12, 23 | |
| 20 | 3, 16 | |
| 21 | 1a, 9 | |
| 22 | 4, 5, 19, 24, 25 | |
| 25 | 1b, 19 | |
| 26 | 12, 19, 23, 24 | |
| 27 | 3, 12, 16 | |
| 30 | 1b, 2, 21, 31 | |
| 32 | 8, 10, 12, 19, 23, 24, 27, 28 | |
| 35 | 3, 6, 12, 16, 29 | |
| 37 | 4, 19, 25 | |
| 38 | 3, 6, 9, 12, 16, 23 | |
| 41 | 1a, 21, 31 | |
| 42 | 3, 6, 12 | |
| 45 | 3, 6, 12, 16 | |
| 58 | 2, 21, 31 | |
| 59 | 4, 25 | |
| pNW | | |
| 1 | 1b, 2, 4, 5, 19, 25 | pHC79 |
| 2 | 3, 7, 15, 20, 22, 29 | |
| 14 | 3, 7, 15, 16, 18, 22, 24 | |
| 21 | 1b, 2, 19, 21, 31 | |
| 29 | 1b, 4, 5, 19, 24, 25 | |
| 44 | 7, 11, 16, 17, 18, 21, 24, 30(doublet), 32, X | |
| 45 | 8, 10, 12, 13, 19, 23, 24, 25, 26, 32 | |
| 52 | 3, 6, 12, 16, 23, 24, 27, 28, 29 | |
| 56 | 3, 5, 15, 20, 22, 24, 29, 33, 34 | |
| 63 | 3, 7, 15, 20, 22, 24, 29, 33, 34 | |
| 68 | 8, 10, 12, 13, 19, 23, 25, 26, 32 | |

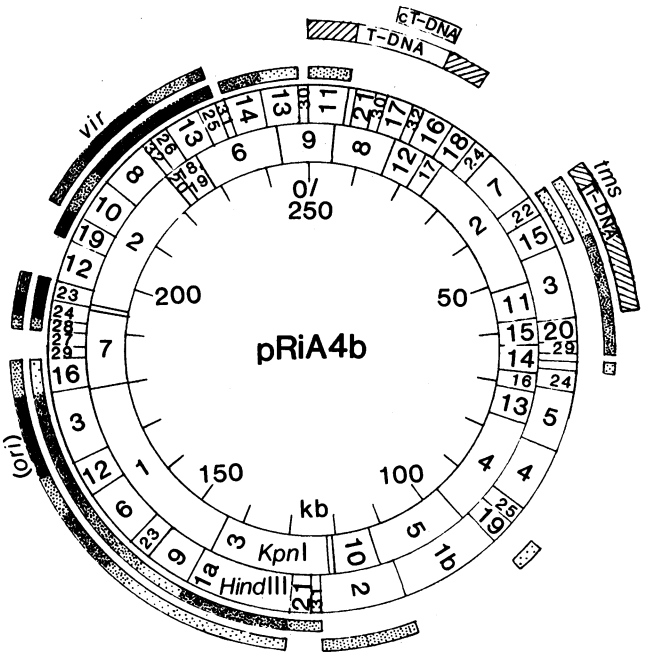


FIG. 2. Restriction map of pRiA4b showing regions of homology to related crown gall plasmids. Shaded arcs represent homology to pTiT37 (inner) and pTiA6 (outer). Relative intensities of Southern blot autoradiogram signals are indicated by the degree of shading. Regions of homology to the specific functions *tms*, *vir*, and the plasmid replication region (*ori*) are noted. T-DNA and homology to *N. glauca* genome cT-DNA are included with cross-hatched ends to indicate the uncertainty of their extent.

Some portions of the plasmid contained too few *Kpn*I sites to establish the fidelity of one or more clones. In these instances, the map was confirmed by hybridization of whole plasmid digests with various $^{32}$P-labeled clones. For example, clone pGH11 (*Hin*dIII fragments 1b, 4, 19, and 25) contained a single *Kpn*I site. Another clone containing *Hin*dIII fragments 1a, 4, 19, and 25 likewise contained a single *Kpn*I site. Several different clones suggested that *Hin*dIII-1a did not map with fragments 4, 19, and 25. We tested this by hybridizing the nonoverlapping clones pGH12 (*Hin*dIII-1a), pGH17 (*Hin*dIII-1b), and pGH22 (*Hin*dIII fragments 4, 5, 19, 24, and 25) to pRiA4b digested with *Bam*HI. Clones pGH17 and pGH22 hybridized to a common *Bam*HI fragment, but pGH12 and pGH22 did not, confirming the location of 1b and not 1a adjacent to the 4-19-25 region.

**DNA homology between pRiA4b and Ti plasmids pTiA6 and pTiT37.** Regions of homology between Ri and Ti plasmids have been identified on the map of octopine- and nopaline-type Ti plasmids (33, 34). To determine where these regions of homology mapped on pRiA4b, we prepared Southern blots from *Hin*dIII digests of pRiA4b and Ri plasmid clones and hybridized them to $^{32}$P-labeled Ti plasmid probes. Under conditions of fairly high stringency, allowing up to about

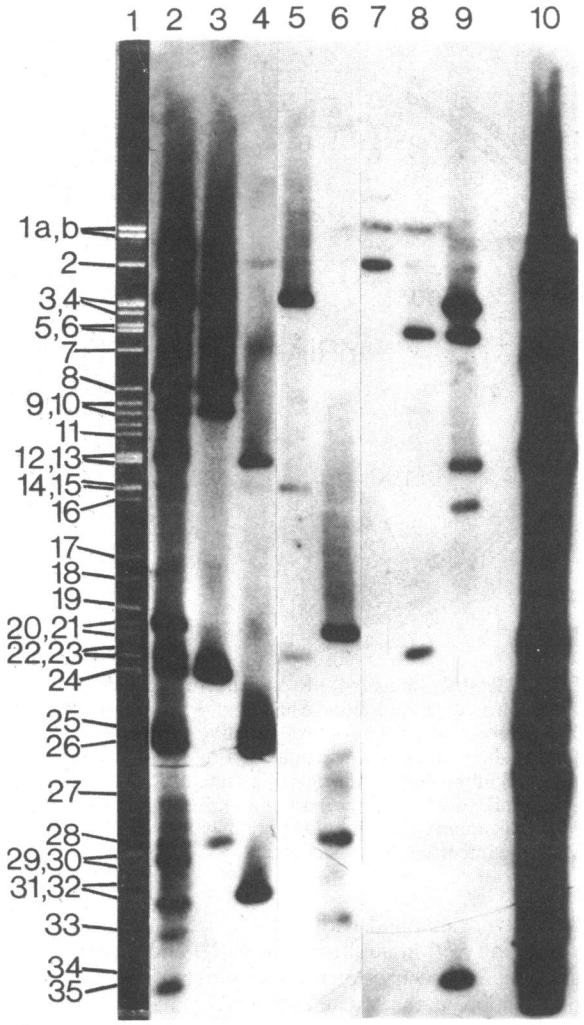


FIG. 3. Southern blot analysis of homology between pRiA4b and pTiA6. Lane 1, electrophoretic pattern of pRiA4b digested with *Hin*dIII. Remaining lanes are autoradiograms of $^{32}$P-labeled pTiA6 hybridized to *Hin*dIII digests of: 2, pRiA4b; 3, pGH32; 4, pFW22; 5, pFW41; 6, pFW55; 7, pGH14; 8, pGH9; 9, pGH35; and 10, pTiA6.

12% mismatch, homology was observed between pRiA4b and the well-characterized octopine-type wide host range plasmid pTiA6 (Fig. 3, lane 2). The most extensive homology was present in the region of pRiA4b represented by the contiguous clones pFW22, pGH32, and pGH35 (Fig. 3, lanes 4, 3, and 9, respectively). Notably, pFW94, which contains the previously observed T-DNA of pRiA4b, had no detectable homology to pTiA6 (data not shown). Hybridization of pTiA6 with itself is shown in Fig. 3, lane 10 for comparison with hybridization of pTiA6 to the Ri plasmid and cloned Ri plasmid fragments. These data are summarized in Fig. 2.

*Hin*dIII digests of pRiA4b and selected clones were also hybridized to the nopaline-type Ti plasmid pTiT37 (Fig. 4). The homology of pTiT37 to pRiA4b was comparable with that between pTiA6 and pRiA4b. Again, the most extensive homology was with clones pFW22, pGH32, and pGH35 (Fig. 4 lanes 4, 3, and 9, respectively), and most of the T-DNA of pRiA4b had no homology with pTiT37. Some homology to pTiT37 was detected with *Hin*dIII-11 at the left end of the T-DNA (Fig. 4, lane 5).

Large segments of pRiA4b appeared to be unrelated to either Ti plasmid on the basis of homology. Nearly half of pRiA4b, the region from coordinates 10 to 120 in Fig. 2, lacked detectable homology to pTiT37, except for a very small amount of homology between coordinates 40 and 50. Large segments of pRiA4b with little or no homology to pTiA6 overlapped the region of low homology to pTiT37 from kilobase coordinates 235 to 40 and 65 to 110. Two segments having a substantial amount of homology with pTiA6 were present in the stretch of pRiA4b lacking homology to pTiT37 (coordinates 47 to 65 and 110 to 122, Fig. 2).

**DNA homology between pRiA4b and the *vir* region of pTiA6.** To define the functional significance of homologous regions to pTiA6 and pTiT37 in pRiA4b, specific Ti plasmid clones were hybridized with pRiA4b or Ri plasmid clones. The *vir* region of pTiA6 has been shown to contain extensive homology to pRiA4b (33). This homology was thought to correspond to the homology to pTiA6 and pTiT37 observed

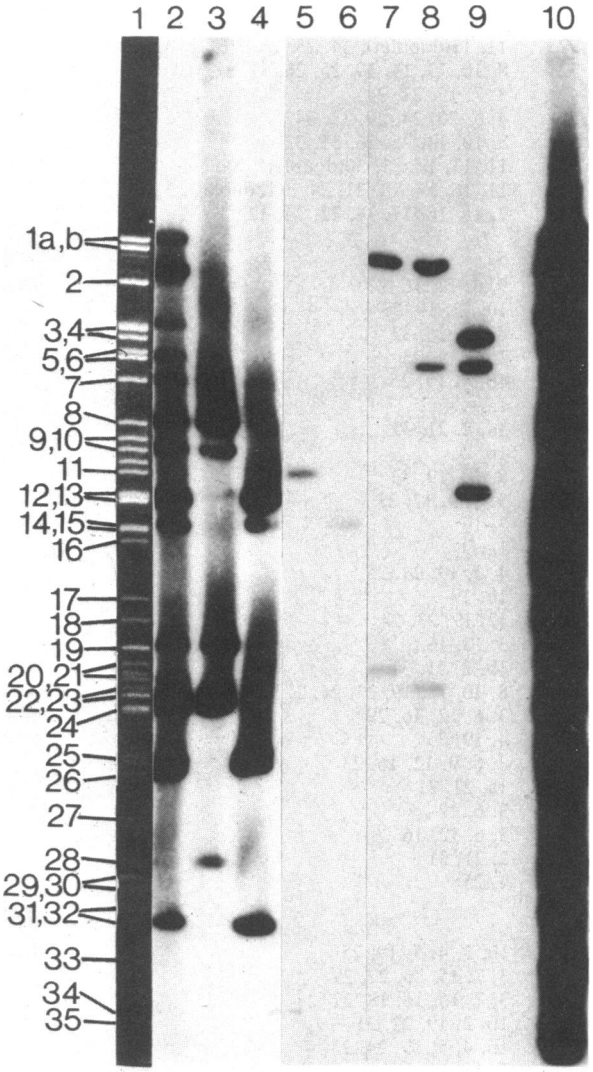


FIG. 4. Southern blot analysis of homology between pRiA4b and pTiT37. Lane 1, electrophoretic pattern of pRiA4b digested with *Hin*dIII. Remaining lanes are autoradiograms of $^{32}$P-labeled pTiT37 hybridized to *Hin*dIII digests of: 2, pRiA4b; 3, pGH32; 4, pFW22; 5, pFW94; 6, pFW41; 7, pGH14; 8, pGH9; 9, pGH35; and 10, pTiT37.

for clones pGH32, pFW22, and possibly pGH35. To test this hypothesis, $^{32}$P-labeled clones containing the *vir* region of pTiA6 were hybridized to a blot of the pRiA4b-derived clones. Homology to the *vir* clone was observed for *Hin*dIII fragments 24, 23, 10, 8, 32, 26, 13, and 25 of the pRiA4b-derived clones pGH32 and pFW22 (Fig. 5, lanes 1 and 2). A second clone containing the end of the *vir* region of pTiA6 closest to the T-DNA of pTiA6 hybridized to *Hin*dIII fragments 25 and 13 (data not shown), indicating that the orientation of the Ri plasmid *vir* homology to the Ri plasmid T-DNA was the same as the orientation of pTiA6 *vir* to the pTiA6 T-DNA.

**DNA homology between pRiA4b and the replication region of pTiA6.** Although the Ri and Ti plasmids are compatible, indicating divergent replication systems, they retain homology in the replication region (33). A clone encompassing the replication region of pTiA6 hybridized to *Hin*dIII fragment 3 of the pRiA4b-derived clone pGH35 (Fig. 5, lane 3). The position of this homology, relative to *vir* homology and T-DNA of pRiA4b, is roughly analogous to that of the pTiA6 origin of replication, relative to *vir* and T-DNA.

**DNA homology between pRiA4b and T-DNA of pTiA6 and pTiT37.** Ti plasmid T-DNA segments were tested for homology to portions of the Ri plasmid by preparing blots of pRiA4b or of clones derived from pRiA4b and hybridizing them to $^{32}$P-labeled clones from the T-DNA of pTiA6 (Fig. 5, lanes 4 through 11). The clones derived from pTiA6 are diagrammed in the lower half of Fig. 5.

*Hin*dIII-18c of pTiA6 (Fig. 5, probe a) encodes T-DNA tumor transcripts 5 and 7 of unknown function. This segment is homologous to pRiA4b *Hin*dIII fragment 19 (Fig. 5, lane 4) at kilobase coordinate 95. *Hin*dIII-22e of pTiA6 (Fig. 5, probe b) encodes the *tms-2* transcript; it hybridized to pRiA4b *Hin*dIII fragment 22 (Fig. 5, lane 5) at kilobase coordinate 40. Clones containing pTiA6 fragments *Hin*dIII-36b or *Bam*HI-30b (Fig. 5, probes c and d) were used as

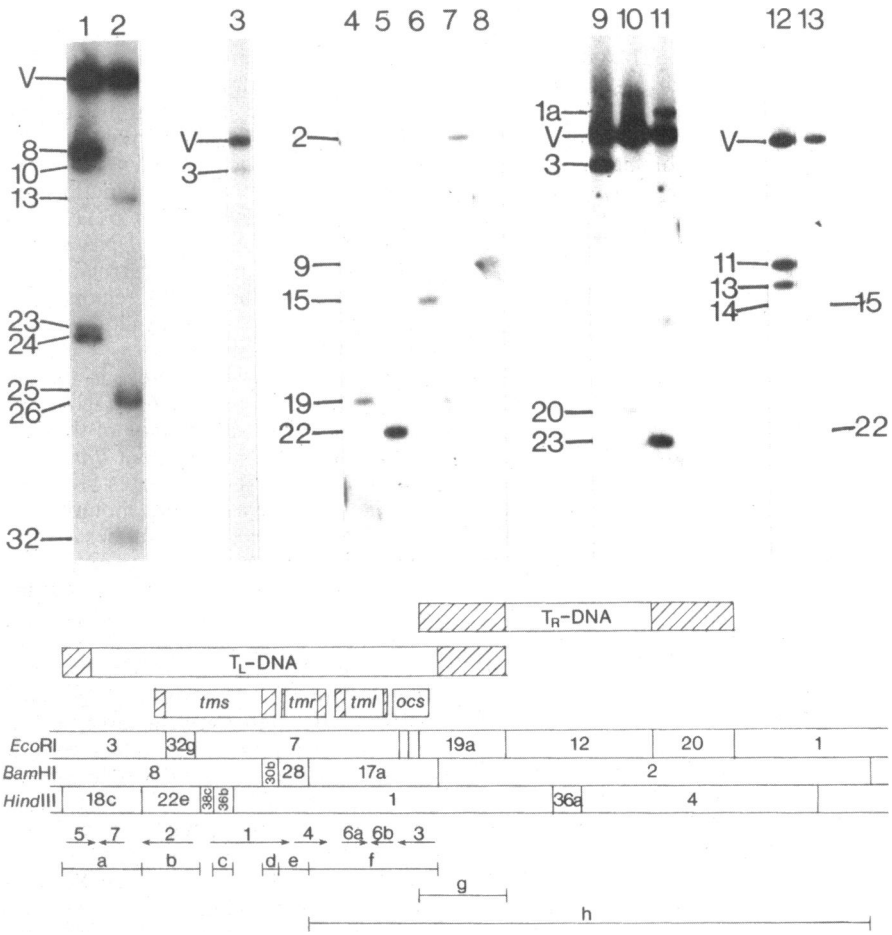


FIG. 5. Southern blot analysis of homology between pRiA4b and specific segments of Ti plasmids. Each lane shows an autoradiogram of a $^{32}$P-labeled cloned Ti plasmid segment (probe) hybridized to *Hin*dIII digests of pRiA4b or a cloned segment of pRiA4b (blot). Bands of homology are numbered according to the *Hin*dIII map of pRiA4b, with vector homology labeled V. Probes used in lanes 4 through 11 are cloned T-DNA segments of pTiA6. These probes are diagrammed on the map of the T-DNA region of pTiA6 below the autoradiograms. Probes are shown by segments labeled a through h. For reference, the tumor morphology loci *tms* (shooty tumor), *tmr* (rooty tumor), and *tml* (large tumor) and the octopine synthesis locus (*ocs*) are shown in bars above the restriction map. The corresponding tumor transcripts from the left hand T-DNA are shown as numbered arrows. $T_L$-DNA, leftward T-DNA; $T_R$-DNA, rightward T-DNA. Lanes: 1 and 2, probe is pHK121 containing the *vir* region of pTiA6 (15), and blots are pGH32 and pFW22, respectively; 3, probe is pVK252 containing the replication region of pTiA6 (16), and blot is pGH35; 4, probe a with blot pGH11; 5, probe b with blot pFW41; 6, probe c with blot pFW41; 7, probe f with blot pRiA4b; 8, probe g with blot pGH9; 9, 10, and 11, probe h with blots pFW41, pFW55, and pGH9, respectively; 12, probe is pNW22B-9, 11, 14-1 (*Bst*EII-9+11+14 from the T-DNA of pTiT37, reference 36), and blot is pFW22; 13, probe is *Bam*HI (9 + 23) from the T-DNA of pTiT37 (35), and blot is pFW41.

specific probes for the *tms-1* locus. Each showed homology to pRiA4b fragment *Hin*dIII-15 (Fig. 5, lane 6), adjacent to the fragment with homology to *tms-2*.

In lane 7 of Fig. 5 hybridization between pRiA4b and *Bam*HI-17a of pTiA6 is shown. This fragment includes part or all of the *tmr*, *tml*, and *ocs* loci (Fig. 5, probe f). It hybridized very faintly to *Hin*dIII fragment 2 of pRiA4b (110 to 125 kb on the map). The signal was unlikely to be due to *tmr* homology, because the pTiA6-derived *Bam*HI-28 fragment (Fig. 5, probe e), which contains half of the *tmr* gene, did not hybridize to pRiA4b (data not shown). We have not ruled out that a fragment of the *tmr* gene having homology to *Bam*HI-17a but not *Bam*HI-28 is present. Alternatively, the homology may correspond to the *tml* locus.

*Eco*RI fragment 19a of pTiA6 (Fig. 5, probe g) includes the *ocs* gene and the right end of the leftward T-DNA. This fragment hybridized slightly to pRiA4b *Hin*dIII fragment 9 (Fig. 5, lane 8) at coordinate 150. The observed homology was not due to *ocs*, since the *Bam*HI-17a fragment of pTiA6, which overlaps *Eco*RI-19a and contains all of *ocs*, hybridized only to *Hin*dIII fragment 2 of pRiA4b. Finally, a clone containing *Bam*HI fragments 2 and 17a of pTiA6 was used as a probe (Fig. 5, probe h, lanes 9 through 11). Homologies detected with this probe but not with *Bam*HI-17a (Fig. 5, probe f, lane 7) were attributed to *Bam*HI-2, which encompasses the rightward T-DNA of pTiA6, including the agropine synthesis (*ags*) and mannopine synthesis (*man*) loci. Homology to *Hin*dIII fragments 1a and 23 (coordinates 130 to 155) and to *Hin*dIII fragments 3 and 20 (coordinates 47 to 62) was observed with probe h but not probe f.

Clones of different parts of the T-DNA of pTiT37 were also hybridized to clones of pRiA4b (Fig. 5, lanes 12 and 13). Homology was observed between the T-DNA region of pTiT37 and the *Hin*dIII fragments 15 and 22 of pRiA4b (Fig. 5, lane 13). This was expected since *tms* is present in the T-DNA of pTiT37. In addition, homology was observed between the leftward T-DNA of pTiT37 and *Hin*dIII fragments 11, 13, and 14 (Fig. 5, lane 12) at the left end of the T-DNA of pRiA4b (coordinates 237 to 6). This homologous region was within a *Kpn*I fragment of pTiT37 (data not shown) which corresponded approximately to a region of Ri plasmid homology previously reported in the closely related nopaline-type plasmid pTiC58 (34).

## DISCUSSION

We have established a physical map for the Ri plasmid pRiA4b, including *Hin*dIII and *Kpn*I restriction sites and regions of homology to two Ti plasmids and specific Ti plasmid loci. The data presented show that as much as 160 kb of pRiA4b had detectable homology to pTiA6, pTiT37, or both. Approximately 33 kb hybridized at high stringency to the *vir* region of pTiA6. Mutagenesis data to be reported elsewhere confirm that this region of pRiA4b includes functions required for virulence of *Agrobacterium rhizogenes*.

One T-DNA region of pRiA4b extends about 15 to 20 kb from *Hin*dIII-11 to *Hin*dIII-16 (31). Homology between this region and either Ti plasmid was limited to *Hin*dIII-11, which contained homology to a segment of T-DNA from pTiT37. Any functions represented by this weak homology have yet to be determined. Mutagenesis data indicate that at least three loci affecting tumor morphology, one of which has been described previously (30), are in the T-DNA of pRiA4b; however, they do not map in *Hin*dIII-11. The homologous region in the T-DNA of pTiT37 is likewise functionally undefined.

The Ri plasmid homology to the *tms* loci of pTiA6 mapped more than 15 kb to the right of the previously identified T-DNA of pRiA4b, suggesting that additional T-DNA might be found in hairy root tumors. In fact, recent evidence has demonstrated that a second Ri plasmid T-DNA region encompasses these homologies in pRiA4b. Near the *tms* homology was a region of pRiA4b having homology to *Bam*HI fragment 2 of pTiA6, which may correspond to the opine synthesis loci *ags* and *man*. Homology to *tmr*, on the other hand, was not detected in this T-DNA segment of pRiA4b.

It is not surprising that *tms* homology should occur in the T-DNA of Ri plasmids, nor that *tmr* homology should be lacking. The rooty phenotype of tumors induced by *A. rhizogenes* is comparable to that of tumors induced by *tmr* mutants of *Agrobacterium tumefaciens*. These observations suggest that similar underlying mechanisms give rise to both phenotypes. Nonetheless, it is highly significant that one T-DNA segment of pRiA4b is completely separate, with no homology to any known tumor morphology locus; yet it encodes tumor morphology functions. This finding implies that a set of previously unknown T-DNA functions exists which affects tumor morphology either independently of or coordinately with the *tms* locus.

Moreover, the T-DNA of pRiA4b includes a segment, the cT-DNA in Fig. 2, with homology to the genome of uninfected *N. glauca* (30). This region, which includes the aforementioned tumor morphology functions, had no detectable homology to either pTiA6 or pTiT37. Spano et al. (25) have identified T-DNA and cT-DNA regions for pRi1855-transformed and uninfected carrots. Similarities between the *Eco*RI map of the T-DNA region in pRi1855 and in pRiA4b (data not shown) suggest that the regions are homologous in these two Ri plasmids.

Another point of interest is that scattered segments of homology to other pTiA6 T-DNA segments were observed in pRiA4b. The significance of these homologies is unclear. The pTiA6 T-DNA fragment *Bam*HI-17a had weak homology to *Hin*dIII-2 at coordinates 110 to 125 of pRiA4b. However, lack of corresponding homology for pTiA6 fragments *Bam*HI-28 or *Eco*RI-19a implies that the observed homology does not correspond to *tmr* or *ocs*. *Hin*dIII-18c of pTiA6, which includes two T-DNA tumor transcripts of unidentified function, hybridized to *Hin*dIII fragment 19 of pRiA4b (coordinate 95). *Bam*HI-2 of pTiA6, which contains the rightward T-DNA of pTiA6, hybridized to pRiA4b at coordinates 47 to 62 and 130 to 155. The scattered homology within pRiA4b to loci that are clustered in the T-DNA of pTiA6 was surprising. If all these regions were involved in the transformation of plant cells, it would entail the transfer into the plant cells of more than one half of the plasmid as a single piece or as many as four smaller separate pieces.

Our data are in agreement with and extend previous reports on homology between Ri and Ti plasmids (33, 34), with one minor difference. Two specific segments of the leftward T-DNA of pTiC58 have been reported to hybridize to the Ri plasmid pRi15834 (34). The nopaline-type Ti plasmids pTiC58 and pTiT37 are closely related, sharing extensive homology in a continuous stretch of DNA except for a ca. 1-kb piece in the T-DNA of pTiC58 not found in pTiT37 (8). One of the segments of pTiC58 hybridizing to pRi15834 includes this 1-kb piece. We did not detect homology to the equivalent segment from pTiT37 in pRiA4b. The region of homology may be reduced in pTiT37 beyond our limits of detection, although we cannot rule out that pRiA4b differs from pRi15834 in this regard.

Another point of passing interest concerns our restriction

map of the Ri plasmid. More recently isolated pRiA4b DNA appeared to have an insertion not previously observed. Earlier preparations of pRiA4b (Fig. 1) contained a doublet *Hin*dIII band 16. In later preparations (Fig. 3), *Hin*dIII-16 was single band, and a new band was observed between *Hin*dIII fragments 10 and 11. The simplest explanation is that an insertion of about 1.4 kb occurred in one of the *Hin*dIII-16 fragments. The clone bank was constructed from earlier preparations of DNA; hence, the new fragment was not observed in any clones, and the map contains two *Hin*dIII-16 fragments at kilobase coordinates 20 and 183.

The mapping of pRiA4b has already proven useful in correlating the data regarding T-DNA and homology to Ti plasmid T-DNA functions. It has also provided some insight into the comparative organization of the Ri and Ti plasmids. Parallel organization at a gross level between the Ri and Ti plasmids is evident in the relative positions of the replication region, the *vir* homology, and one T-DNA region. However, differences in the organization of T-DNA loci on the plasmid and degree of relatedness are striking. More detailed examination of the T-DNA regions will be facilitated by the existing map and availability of clones of these regions.

## ACKNOWLEDGMENTS

We thank R. Finical and K. Spangler for typing the manuscript and C. Lichtenstein, A. Montoya, H. Klee, and V. Knauf for plasmids, assistance, and useful discussions.

This work was supported by Public Health Service grant CA-13015 from the National Cancer Institute. G.A.H. and F.F.W. are postdoctoral fellows supported by Public Health Service grant CA-07017 from the National Cancer Institute and National Science Foundation grant PDF8166050, respectively.

## LITERATURE CITED

1. **Birnboim, H. C., and J. Doly.** 1979. A rapid alkaline extraction procedure for screening recombinant plasmid DNA. Nucleic Acids Res. **7**:1513–1523.
2. **Blattner, F. R., B. G. Williams, A. E. Blechl, K. Denniston-Thompson, H. E. Faber, L.-A. Furlong, D. J. Grunwald, D. O. Kiefer, D. D. Moore, J. W. Schumm, E. L. Sheldon, and O. Smithies.** 1977. Charon phages: safer derivatives of bacteriophage lambda for DNA cloning. Science **196**:161–169.
3. **Boyer, H. W., and D. Roulland-Dussoix.** 1969. A complementation analysis of the restriction and modification of DNA in *Escherichia coli*. J. Mol. Biol. **41**:459–472.
4. **Chilton, M.-D., M. H. Drummond, D. J. Merlo, D. Sciaky, A. L. Montoya, M. P. Gordon, and E. W. Nester.** 1977. Stable incorporation of plasmid DNA into higher plant cells: the molecular basis of crown gall tumorigenesis. Cell. **11**:263–271.
5. **Chilton, M.-D., D. A. Tepfer, A. Petit, C. David, F. Casse-Delbart, and J. Tempé.** 1982. *Agrobacterium rhizogenes* inserts T-DNA into the genomes of the host plant root cells. Nature (London) **295**:432–434.
6. **Currier, T. C., and E. W. Nester.** 1976. Isolation of covalently closed circular DNA of high molecular weight from bacteria. Anal. Biochem. **76**:431–441.
7. **Denhardt, D. T.** 1966. A membrane-filter technique for the detection of complementary DNA. Biochem. Biophys. Res. Commun. **23**:641–646.
8. **Depicker, A., M. De Wilde, G. De Vos, R. De Vos, M. Van Montagu, and J. Schell.** 1980. Molecular cloning of overlapping segments of the nopaline Ti-plasmid pTiC58 as a means to restriction endonuclease mapping. Plasmid **3**:193–211.
9. **Enquist, L., and N. Sternberg.** 1979. *In vitro* packaging of λ *Dam* vectors and their use in cloning DNA fragments. Methods Enzymol. **68**:281–298.
10. **Garfinkel, D. J., R. B. Simpson, L. W. Ream, F. F. White, M. P. Gordon, and E. W. Nester.** 1981. Genetic analysis of crown gall: fine structure map of the T-DNA by site directed mutagenesis. Cell **27**:143–153.
11. **Guyon, P., M.-D. Chilton, A. Petit, and J. Tempé.** 1980. Agropine in "null-type" crown gall tumors: evidence for generality of the opine concept. Proc. Natl. Acad. Sci. U.S.A. **77**:2693–2697.
12. **Hernalsteens, J. P., H. De Greve, M. Van Montagu, and J. Schell.** 1978. Mutagenesis by insertion of the drug resistance transposon Tn7 applied to the Ti plasmid of *Agrobacterium tumefaciens*. Plasmid **1**:218–225.
13. **Hohn, B., and J. Collins.** 1980. A small cosmid for efficient cloning of large DNA fragments. Gene **11**:291–298.
14. **Holsters, M., B. Silva, F. Van Vliet, C. Genetello, M. De Block, P. Dhaese, A. Depicker, D. Inzé, G. Engler, R. Villarroel, M. Van Montagu, and J. Schell.** 1980. The functional organization of the nopaline *A. tumefaciens* plasmid pTiC58. Plasmid **3**:212–230.
15. **Klee, H. J., M. P. Gordon, and E. W. Nester.** 1982. Complementation analysis of *Agrobacterium tumefaciens* Ti plasmid mutations affecting oncogenicity. J. Bacteriol. **150**:327–331.
16. **Knauf, V. C., and E. W. Nester.** 1982. Wide host range cloning vectors: a cosmid clone bank of an *Agrobacterium* Ti plasmid. Plasmid **8**:45–54.
17. **Maniatis, T., A. Jeffrey, and D. G. Kleid.** 1975. Nucleotide sequence of the rightward operator of phage lambda. Proc. Natl. Acad. Sci. U.S.A. **72**:1184–1188.
18. **Miller, J. H.** 1972. Experiments in molecular genetics, p. 433. Cold Spring Harbor Laboratory, Cold Spring Harbor, N.Y.
19. **Moore, L., G. Warren, and G. Strobel.** 1979. Involvement of a plasmid in the hairy root disease of plants caused by *Agrobacterium rhizogenes*. Plasmid **2**:617–626.
20. **Ooms, G., P. M. Kapwijk, J. A. Poulis, and R. A. Schilperoort.** 1980. Characterization of Tn*904* insertions in octopine Ti plasmid mutants of *Agrobacterium tumefaciens*. J. Bacteriol. **144**:82–91.
21. **Petit, A., C. David, G. A. Dahl, J. G. Ellis, P. Guyon, F. Casse-Delbart, and J. Tempé.** 1983. Further extension of the opine concept: plasmids in *Agrobacterium rhizogenes* cooperate for opine degradation. Mol. Gen. Genet. **190**:204–214.
22. **Riker, A. J., W. M. Banfield, W. H. Wright, G. W. Keitt, and H. E. Sagen.** 1930. Studies on infectious hairy-root of nursery apple trees. J. Agric. Res. (Washington, D.C.) **41**:507–540.
23. **Scott, I. M., J. L. Firmin, D. N. Butcher, L. M. Searle, A. K. Sogeke, J. Eagles, J. F. March, R. Self, and G. R. Fenwick.** 1979. Analysis of a range of crown gall and normal plant tissues for Ti plasmid-determined compounds. Mol. Gen. Genet. **176**:57–65.
24. **Southern, E. M.** 1975. Detection of specific sequences among DNA fragments separated by gel electrophoresis. J. Mol. Biol. **98**:503–517.
25. **Spano, L., M. Pomponi, P. Constantino, G. M. S. Van Slogteren, and J. Tempé.** 1982. Identification of T-DNA in the root-inducing plasmid of the agropine type *Agrobacterium rhizogenes* 1855. Plant Mol. Biol. **1**:291–300.
26. **Tepfer, D. A., and J. Tempé.** 1981. Production d'agropine par des racines formées sous l'action d'*Agrobacterium rhizogenes* souche A4. C. R. Acad. Sci. Ser. III **292**:153–156.
27. **Thomashow, M. F., R. Nutter, A. L. Montoya, M. P. Gordon, and E. W. Nester.** 1980. Integration and organization of Ti plasmid sequences in crown gall tumors. Cell **19**:729–739.
28. **Van Larebeke, N., G. Engler, M. Holsters, S. Van den Elsacker, I. Zaenen, R. A. Schilperoort, and J. Schell.** 1974. Large plasmid in *Agrobacterium tumefaciens* essential for crown gall-inducing ability. Nature (London) **252**:169–170.
29. **Watson, B., T. C. Currier, M. P. Gordon, M.-D. Chilton, and E. W. Nester.** 1975. Plasmid required for virulence of *Agrobacterium tumefaciens*. J. Bacteriol. **123**:255–264.
30. **White, F. F., D. J. Garfinkel, G. A. Huffman, M. P. Gordon, and E. W. Nester.** 1983. Sequences homologous to *Agrobacterium rhizogenes* T-DNA in the genomes of uninfected plants. Nature (London) **301**:348–350.
31. **White, F. F., G. Ghidossi, M. P. Gordon, and E. W. Nester.** 1982. Tumor induction by *Agrobacterium rhizogenes* involves the transfer of plasmid DNA to the plant genome. Proc. Natl. Acad. Sci. U.S.A. **79**:3193–3197.
32. **White, F. F., and E. W. Nester.** 1980. Hairy root: plasmid

encodes virulence traits in *Agrobacterium rhizogenes*. J. Bacteriol. **141**:1134–1141.
33. **White, F. F., and E. W. Nester.** 1980. Relationship of plasmids responsible for hairy root and crown gall tumorigenicity. J. Bacteriol. **144**:710–720.
34. **Willmitzer, L., J. Sanchez-Serrano, E. Buschfeld, and J. Schell.** 1982. DNA from *Agrobacterium rhizogenes* is transferred to and expressed in axenic hairy root plant tissues. Mol. Gen. Genet. **186**:16–22.
35. **Yadav, N. S., K. Postle, R. K. Saiki, M. F. Thomashow, and M.-D. Chilton.** 1980. T-DNA of a crown gall teratoma is covalently joined to host plant DNA. Nature (London) **287**:458–461.
36. **Yang, F., and R. B. Simpson.** 1981. Revertant seedlings from crown gall tumors retain a portion of the bacterial Ti plasmid DNA sequences. Proc. Natl. Acad. Sci. U.S.A. **78**:4151–4155.